

On the use of a Raman spectroscopy band to assess the crystalline lateral packing in polyethylene

J. M. LAGARON

*Institute of Agrochemistry and Food Technology, C.S.I.C., Apdo. Correos 73,
46100 Burjassot (Valencia), Spain
E-mail: lagaron@iata.csic.es*

In this study, a thorough analysis of the changes in position of the so-called Raman crystallinity band of polyethylene, i.e., 1415 cm^{-1} Raman band, as a function of temperature, cold-drawing and material density and its interpretation are presented. This Raman band is thought to mainly arise from an interchain interaction, often termed factor group splitting, within the polyethylene orthorhombic lattice and its intensity is widely used to estimate the core orthorhombic crystallinity. The results gathered here support the additional use of this band as an original tool to gain insight into the chain lateral packing of the orthorhombic unit cell, and hence to assess the health of the orthorhombic polyethylene crystals. © 2002 Kluwer Academic Publishers

1. Introduction

It is well-known that polyethylene usually crystallises in an orthorhombic lattice (space group Pnam-No.62 or D_{2h}^{16} in Schoenflies nomenclature) which contains two chains per unit cell with different orientation with respect to each other [1]. The vibrational interaction between these two chains present in the orthorhombic unit cell results in splitting of single-chain Raman and IR active modes. This splitting can be predicted by group theory and hence this phenomenon is often termed factor group splitting. In the case of polyethylene, factor group splitting is only observed at room temperature in the $-\text{CH}_2-$ bending vibrations (Raman and IR active) and in the $-\text{CH}_2-$ rocking (IR active) modes. These molecular vibrations are thought to result in a more intense interchain interaction in the crystals than other molecular vibrations because they involve motions predominantly perpendicular to the chain direction. Factor group splitting effects have also been observed in the vibrational spectra of other polymers like orthorhombic polyoxymethylene [2], aliphatic polyketones [3], etc. Nevertheless, the factor group splitting occurrence is only predicted in crystalline polymorphs with multiple chains per unit cell. Thus, the hexagonal form of polyoxymethylene contains only one chain per unit cell and therefore does not result in factor group splitting. Monoclinic and hexagonal polyethylene can be obtained at high pressure and at high pressure and high temperature respectively, and neither of both result in factor group splitting [4]. Consequently, in the polyethylene case only orthorhombic crystals contribute to give rise to this spectroscopic phenomenon.

A combination of a factor group splitting together with a complex spectroscopic phenomenon called Fermi resonance is thought to give rise to the complex

band shape seen in the Raman $-\text{CH}_2-$ bending range ($1400\text{--}1500\text{ cm}^{-1}$) of the polyethylene Raman spectrum [2]. Thus, a $-\text{CH}_2-$ bending factor group splitting phenomenon, i.e., correlation splitting of single-chain $-\text{CH}_2-$ bending Raman-active mode (A_g) into two components (A_g and B_{1g}) in the crystal, is thought to give rise to the observed bands at ca. 1415 (often called Raman crystallinity band) and 1440 cm^{-1} in polyethylene. The fact that the separation between the components of the Raman $-\text{CH}_2-$ bending splitting, 1415 and 1440 cm^{-1} bands, is so high (around 25 cm^{-1}) in polyethylene is unusual, and it is thought to be caused by the simultaneous presence of the cited Fermi effect which enhances the separation. Although, a more recent study [5] based on the analysis of Stokes and anti-Stokes Raman signals in a high density polyethylene confirms that combination of bands and Fermi resonance are affecting this spectral range, as suspected, it is recognised that a strong component of this band arises from orthorhombic crystalline polyethylene. In fact there is a large body of experimental evidence that indicates that the 1415 cm^{-1} band is dominated by the A_g symmetry component of the predicted factor group splitting in orthorhombic crystalline polyethylene [6 and therein]. Thus, a careful analysis of this $-\text{CH}_2-$ bending range can be a very useful tool to gain qualitative and quantitative information about the crystalline phase of polyethylene. As the 1415 cm^{-1} band (A_g) is thought to arise only in the orthorhombic crystals, Strobl and Hagedorn [7] cleverly proposed a methodology that makes use of the relative intensity of this band to determine the structural phases of isotropic (orthorhombic) polyethylene. Moreover as isotropic polyethylene is mainly orthorhombic the Raman crystallinity as determined by the use of this band is thought

to give a good estimation of the polymer crystallinity content. The method determines crystallinity, amorphous and interfacial content by curve fitting of the experimental spectrum. Although some discussion remains open as to the use of the above method to determine the interfacial content [8], the calculation of orthorhombic crystallinity has been well accepted and widely used. A modification of the above method has also been proposed to overcome molecular orientation in stretched high density polyethylene (HDPE) and calculate the Raman (orthorhombic) crystallinity. In addition to the above, recent works [6, 9] strongly support that the position of this band can also yield relevant information concerning the chain packing efficiency (crystalline density) of the polyethylene crystals.

We report in this paper on a thorough analysis of the band-shift undergone by the Raman crystallinity band, i.e., the $-\text{CH}_2-$ bending 1415 cm^{-1} Raman band, as a function of temperature, cold-drawing and polymer density, and on the interpretation of the latter shift in terms of alterations in the crystalline morphology present in a range of polyethylene materials.

2. Experimental

2.1. Samples

A number of different polyethylene samples were used in this study, for which some physical characteristics are detailed in Table I. All samples were compression moulded by holding pellet material at ca. 60°C above the maximum of melting for five minutes and then cooled under pressure at $20^\circ\text{C}/\text{min}$ in a hot plate press. The cold-drawing process was carried out on dumb-bell shaped specimens (with dimensions $20 \times 4 \times 0.5\text{ mm}$) in a Zwick 1455 stretching device at a constant speed of $10\text{ mm}/\text{min}$ until the full gauge length of the dumb-bell was necked (up to the samples natural draw ratio). The dumb-bell specimens were conditioned prior to testing in boiling water for 30 minutes and subsequent cooling down in water for 16 hours to remove residual stresses and impurities. The melting points summarised in Table I were measured by DSC (Mettler TA 4000) at a heating speed of $10^\circ\text{C}/\text{min}$ and the melting endotherms were reported and discussed in [9].

2.2. Raman experiments

The micro-Raman experiments were carried out with the confocal “LabRam” system of Dilor (France, SA) with 532 nm excitation source (HeNe) which provides typically 16 mW at the sample (further details of this setup can be found in [9]). A heating stage (Linkam TH600) with accuracy in temperature control of $\pm 0.1^\circ\text{C}$ was attached to the latter Raman equipment

to conduct step wise Raman experiments as a function of temperature.

Curve fitting of the experimental profiles was carried out with the Grams Research 2000 software package from Galactic industries. Voigt (convolution of Lorentzian and Gaussian) profiles, no restrictions, and linear baseline conditions were utilized. Fig. 1 shows a typical example of deconvolution of the polyethylene $-\text{CH}_2-$ bending Raman range.

3. Results and discussion

3.1. Temperature effect

In an early paper, Koenig and Boerio [10], found that when a polyethylene sample was measured by Raman at subambient temperature (-160°C) the components of the $-\text{CH}_2-$ bending splitting were seen to separate further apart from each other, i.e., the Raman crystallinity band positioned at 1418 cm^{-1} at room temperature shifted to 1414 cm^{-1} whereas the 1441 cm^{-1} band shifted to 1442 cm^{-1} . This effect is classically attributed to cooling-induced enhanced interchain interaction, which results in larger splitting separation. However, the interesting observation to the purpose of this paper is not only the larger separation of the $-\text{CH}_2-$ splitting components upon cooling but that the splitting components-shift is found to be considerably larger for the Raman crystallinity band, that is ca. 4 cm^{-1} for the Raman crystallinity band vs. 1 cm^{-1} for the so-called 1440 cm^{-1} band. This band shift results, assuming a linear response with temperature, in an “apparent” Raman coefficient of thermal expansion of ca. $0.022\text{ cm}^{-1}/^\circ\text{C}$ for the crystallinity band vs. only $0.0055\text{ cm}^{-1}/^\circ\text{C}$ for the 1440 cm^{-1} band. From this observation, it is clear that it is the former band the most sensitive one to changes in the orthorhombic lattice of the crystalline phase as sensed by the resulting changes in the factor group splitting phenomenon.

Fig. 2 shows that upon heating of a polyethylene sample (PE1) to the melting point, the 1415 cm^{-1} band decreases intensity, particularly at the higher temperatures, and shifts towards higher wavenumber. The drop in intensity as the sample approaches the maximum of melting is probably due to the progressive melting of lower melting point (smaller/defective) crystals. At the maximum of melting, i.e., sample melting point, the band seems to have already vanished. Interestingly, the band concomitantly shifts towards higher wavenumber. This observation points to a weakening of the factor group splitting phenomenon in the orthorhombic crystals induced by heating. Fig. 3 shows that the shift towards higher wavenumber of the crystallinity band appears to follow a linear trend with increasing

TABLE I Some sample characteristics of the polyethylene materials used

Material	PE1	HDPE	LDPE	LLDPE	MPE1 (Metallocene)	MPE2 (Metallocene)
Density (Kg/m^3)	905	953	923	918	903	885
M_w	–	79800	68000	82000	80800	90600
M_w/M_n	–	3.3	3.3	3.4	2.2	2.0
Melting point ($^\circ\text{C}$)	85	130	111	125	101	82

All materials except PE1 (ethylene-1-butene) and LDPE are ethylene-1-octene copolymers. PE1 was kindly supplied by DSM (The Netherlands) and the others by Dow Iberica (Spain).

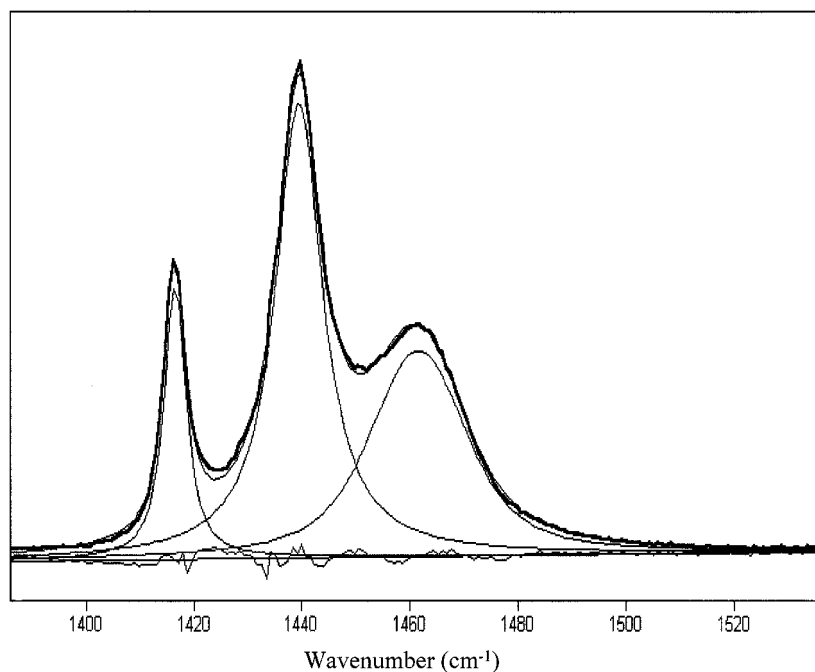


Figure 1 Typical curve-fitting of the Raman $\text{—CH}_2\text{—}$ bending range of polyethylene.

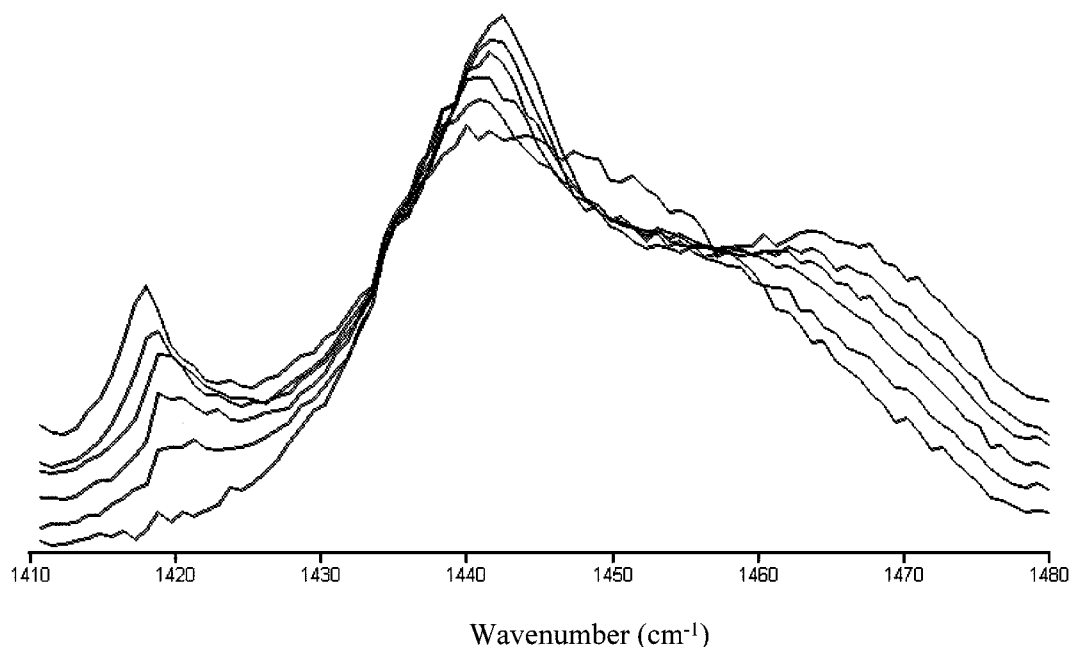


Figure 2 Raman spectra in the $\text{—CH}_2\text{—}$ bending range as a function of temperature (recorded at, from top to bottom, -50 , -10 , 30 , 50 , 70 , 85°C) of an ethylene-1-butene copolymer (PE1).

temperature for this material. This band therefore shifts around 4 cm^{-1} in the temperature range going from -40 to 80°C . As the band shift is thought to be mainly associated with the thermal expansion of the unit cell before melting, effect that results in decreased interchain interaction and hence in decreased intensity of the splitting, by linear regression fitting of the band shift as a function of temperature an “apparent” Raman coefficient of thermal expansion of $0.026\text{ cm}^{-1}/^\circ\text{C}$ can be determined for this polyethylene. This value is slightly higher, but of similar order, than the one estimated from the work of Boerio and Koenig [10]. It is expected that different polyethylene samples will have somewhat different dependency of the band shift with temperature because of

the different morphology of their crystals. Thus, the inclusion of methyl side chains in the crystals, different crystal surface dilatometric stresses, different crystal size distributions and morphologies may surely induce different and measurable temperature behaviour. These effects are being investigated under heating and cooling at present. It is worth noticing that the cited band seems to disappear at around the maximum of melting. As the endset of melting provided by the manufacturer is at 110°C , it appears that the Raman crystallinity band vanishes before the total crystallinity melts away. This observation suggests (see later in text) that below a critical crystalline density, i.e., unit cell interchain distance, the factor group splitting phenomenon, and hence

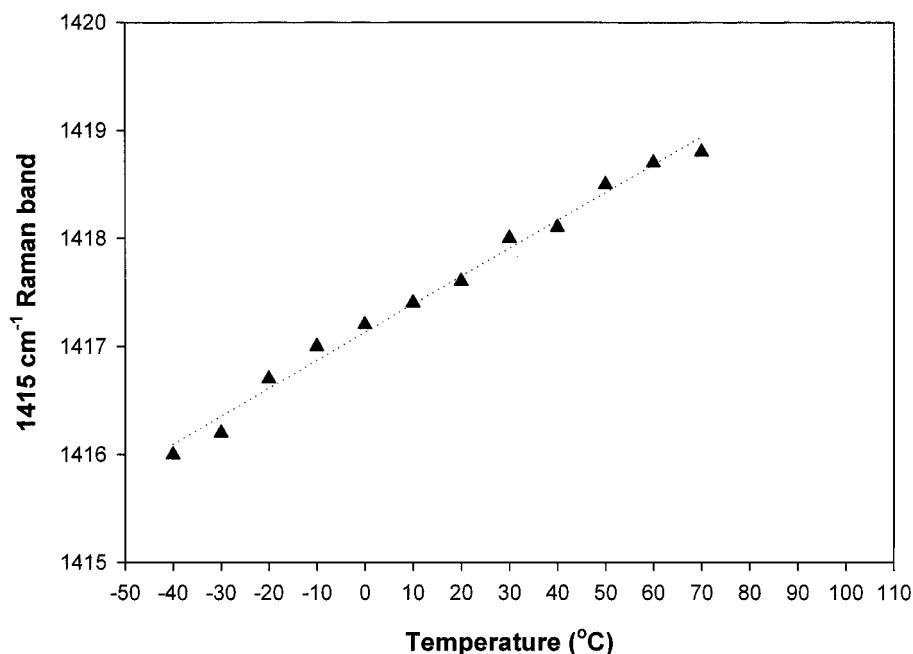


Figure 3 Position of the Raman crystallinity band as a function of temperature for sample PE1.

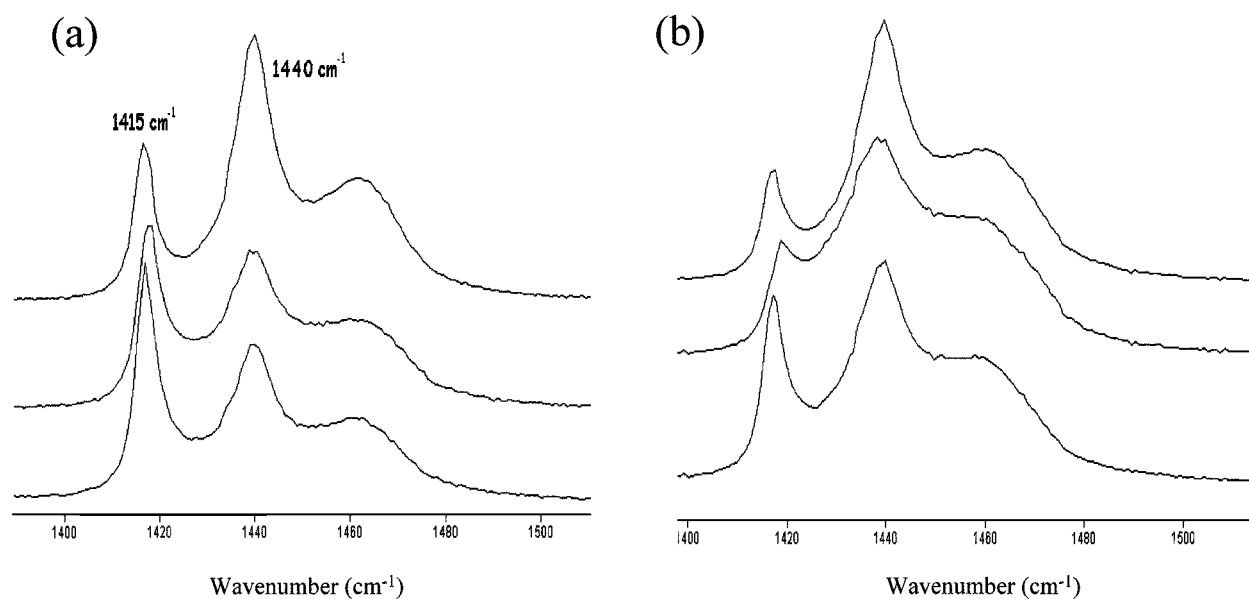


Figure 4 Raman spectrum in the range of the $\text{-CH}_2\text{-}$ bending of, from top to bottom, isotropic, cold-drawn and annealed cold-drawn specimens of (a) HDPE and (b) LDPE. The spectra are normalised to the intensity of the 1295 cm^{-1} internal standard band.

its sensitivity to determine crystallinity in the polymer, cancels. Nevertheless, variations in the intensity of this band could also be ascribed to the band intensity temperature dependence of a Fermi resonance contribution as suggested by Meier *et al* [5].

3.2. Cold-drawing effect

The cold-drawing process is known to induce significant structural changes in polyethylene [11, 12], i.e., molecular orientation in the straining direction, crystal fractionation, solid-solid phase transformation [13, 14] and increased unit cell volume (lower crystalline density). The analysis of the factor group splitting in the Raman spectrum of polyethylene proves to be sensitive to all these effects when analysed with sufficient care [8]. Fig. 4 shows the $\text{-CH}_2\text{-}$ bending range of

isotropic, cold-draw and annealed cold-draw specimens (annealed for 1 hour at a temperature about 20°C below the polymer melting point) of a high density polyethylene sample (HDPE in Table I) and of a low density polyethylene sample (LDPE in Table I). This figure shows that upon cold-drawing significant changes in relative intensity occur in this Raman range. These alterations are in part attributed to molecular orientation effects due to the specific symmetry of the bands involved, but are also due, based on previous research [8], to reductions in orthorhombic crystallinity and solid-solid phase transformation to monoclinic phase. However, the relevant observation to this study is the clear shift of the Raman crystallinity band towards higher wavenumber upon straining. Fig. 5 shows the curve-fit Raman crystallinity band for samples HDPE and LDPE before and after cold-drawing. From this figure

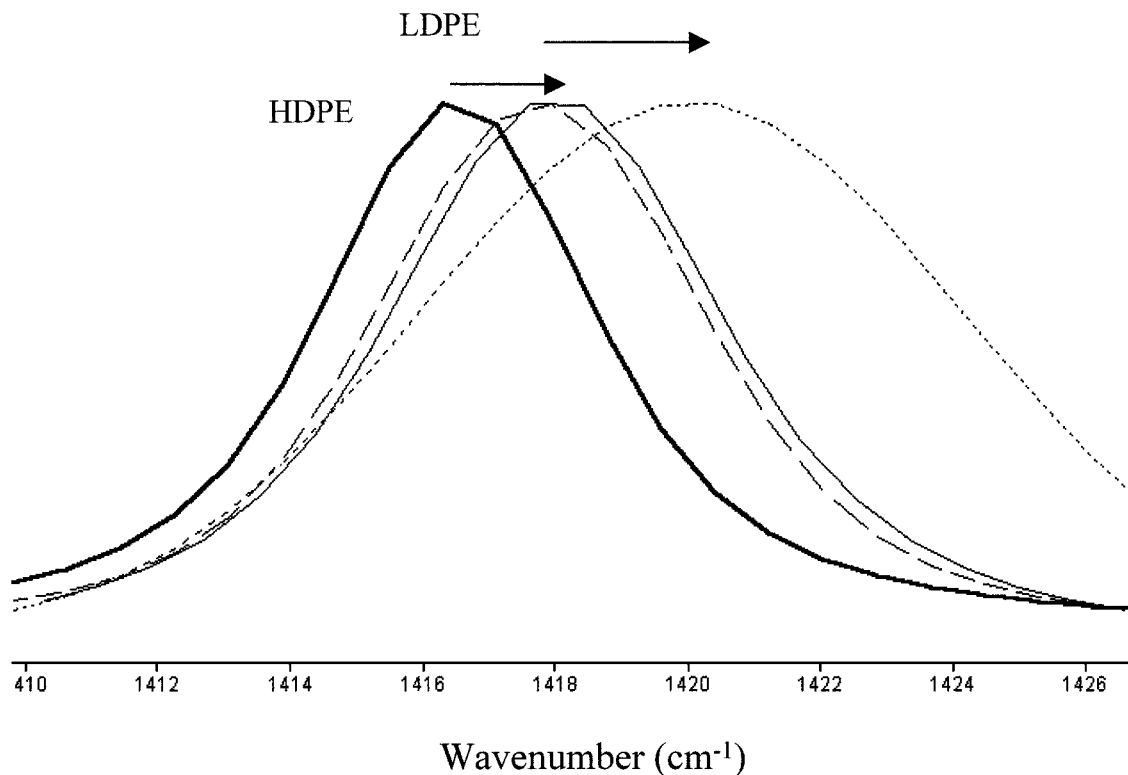


Figure 5 Curve-fitted Raman crystallinity band of isotropic HDPE (thick line), cold-drawn HDPE (thin line), isotropic LDPE (dashed line) and cold-drawn LDPE (dotted line).

it can also be seen that the extent of the shift is material dependent. Thus, the band shift is higher (and the band broader) for LDPE than for HDPE, i.e., 2.3 cm^{-1} for the LDPE vs 1.5 cm^{-1} for the HDPE. This band shift is here again attributed to reductions in lattice interchain interaction due to cell expansion. The latter observations are therefore in agreement with X-ray results: This technique points to a decrease in crystal size (crystal fractionation) and crystalline density (lattice expansion) upon cold drawing [11, 12]. The decrease in crystalline density is due to the increase of chiefly “*a*” but also “*b*” lattice parameters. This indicates that the interacting chains are further apart in the unit cell, effect that must cause depletion in the factor group splitting and hence the 1415 cm^{-1} band-shift towards higher wavenumber cited above. Another interesting observation here is that the position of the crystallinity band is at a higher wavenumber (and broader) for isotropic (undeformed) LDPE than for isotropic HDPE. In real fact, the position of this band in the LDPE is around that of the band in the cold-drawn HDPE. This clearly suggests that crystalline density or unit cell interchain distances could be in average of the same order for both structures and confirms further the observation that cold-drawing results in an ill-defined orthorhombic crystallinity. Of course, upon cold-drawing of the LDPE a higher band shift and band broadening is observed possibly due to long chain branches being pull through the crystals leaving a more distorted and heterogeneous population of crystal sizes and densities. Upon annealing, the orthorhombic crystallinity is recovered towards the flawlessness of the isotropic crystals, hence the observed band intensity rise and the recovery of its original position.

It is relevant to add here that observations of factor group splitting alterations as a result of temperature changes and cold-drawing, which can be rationalized on the same interchain interaction bases, are not limited to the Raman crystallinity band dealt with in this study but have also been also observed, albeit to a lower extent, in other vibrational modes (fundamental modes) where no mixing influence from combination bands and Fermi resonance is suspected. These are the Raman active 1060 cm^{-1} anti-symmetric C–C stretching band and 1295 cm^{-1} –CH₂– twisting band, and the IR active –CH₂– bending and rocking bands [6 and therein].

As a consequence of all the above, the splitting phenomenon, and more particularly the position of the Raman crystallinity band, seems to be a valid tool to assess changes in chain packing within orthorhombic crystals in response to temperature and straining effects. Nevertheless, it would also be interesting to investigate whether this spectroscopic phenomenon could be intense enough to discriminate isotropic samples at room temperature as a consequence of their particular molecular architecture and density.

3.3. Molecular architecture and density effects

To check the influence of density and molecular architecture in the Raman –CH₂– bending splitting a number of isotropic polyethylene grades varying in these characteristics (see Table I) were studied by Raman. From previous work [9], the Raman crystallinity (calculated using the 1415 cm^{-1} band) [6] of these samples was found to decrease more rapidly with decreasing polymer density than crystallinity by other techniques

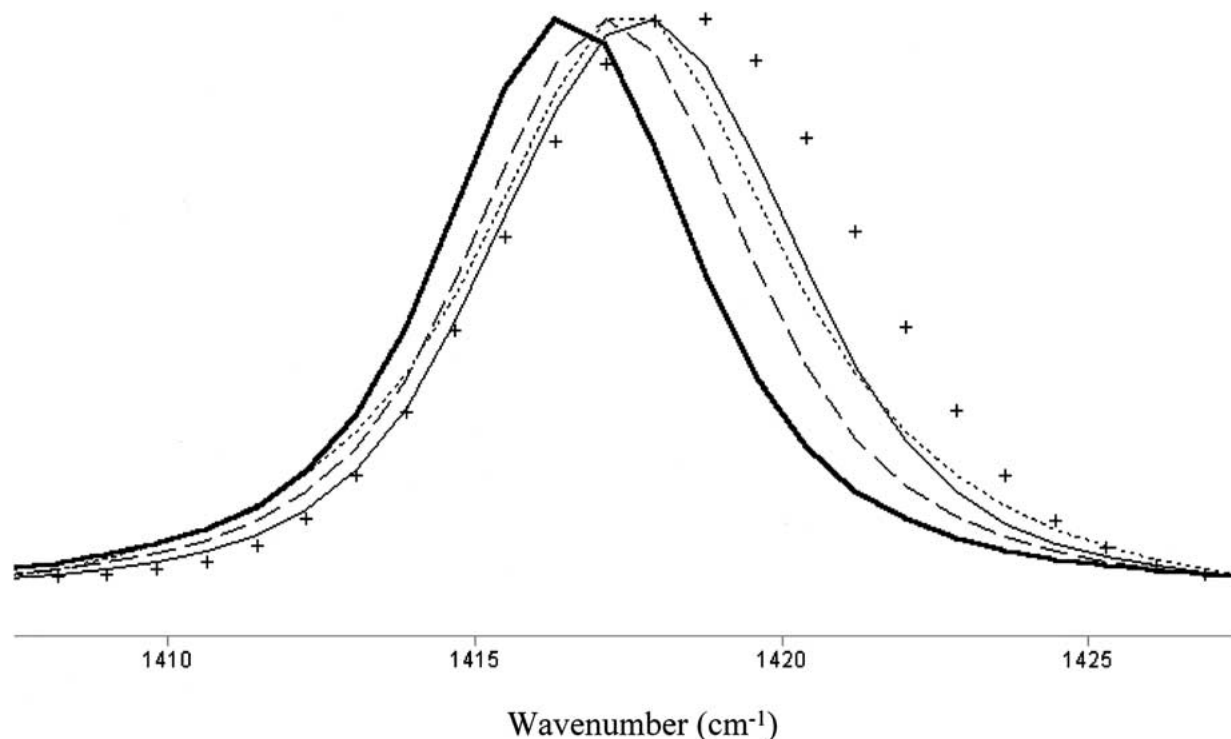


Figure 6 Curve-fitted Raman crystallinity band of isotropic HDPE (thick line), LLDPE (dashed line), MPE1 (dotted line), LDPE (thin line), MPE2 (crosses line).

like DSC and WAXS. This trend has independently been confirmed more recently in a study by Neway *et al.*[15] carried out on a larger number of homogeneous and heterogeneous polyethylene materials. We attributed this observation to the presence of an increased number of crystals with defects and a critical drop in crystalline density, perhaps with different crystalline morphology (hexagonal phase), with decreasing sample density, which do not result in observable factor group splitting.

Fig. 6, shows the curve-fit Raman crystallinity band for the various samples. Instrumental frequency shifts were ruled out by observing that the position of the 1295 cm^{-1} sharp feature of the internal standard Raman range ($-\text{CH}_2-$ twisting range) did not shift across density. From this figure it can be observed that the position of this band is at the lowest wavenumber for the HDPE and at the highest for the metallocene MPE2 sample. The clear differences observed in the position of this band could indicate that interchain distances within crystals differ for the materials as one could expect from the large variations in the molecular architecture and density of the samples. Therefore, the position of this band appears to be sensitive enough to detect changes in the undeformed samples as an overall band shift of about 2 cm^{-1} is measured between the highest and the lowest density sample. However, the band shift does not appear to be consistent with simply the change in sample density as should be expected from the rationalization of the significant differences in the molecular architectures of these materials (see Fig. 7). Fig. 7 plots the position of this band and the maximum of melting (melting point) as a function of density. From this plot there is neither a linear dependency of the shift of this band with density nor of the melting point. The lack of linearity of the

melting point with density is due to the well-known different molecular architecture of the materials studied here, i.e., heterogeneous (particularly Ziegler-Natta linear low density polyethylenes, LLDPE) vs. homogeneous (metallocene polyethylenes) incorporation of side-chains along molecules and across the molecular weight. Metallocene polyethylenes result in a larger depletion of the maximum of melting than heterogeneous materials for the same comonomer incorporation and for the same density because side chains are more randomly distributed both intra- and inter-molecularly, hence the term homogeneous polyethylenes. LLDPE's are known to have a distribution of crystal sizes due to heterogeneous dispersion of the side chains along and across the polymer chains and often exhibit multiple melting point features, hence the term heterogeneous. Further discussion on this can be found in [9]. From this Fig. 7, it is worth noting the reasonable similar trend between the shift of this band with decreasing density and that of the inverse of the melting point. Thus, the Raman crystallinity band seems to be able to pick up differences in the molecular structure exhibited by the different samples in a trend similar to the inverse melting point. The band shift towards higher wavenumber with decreasing melting point and density could reflect that the orthorhombic crystals giving rise to this band do have an increased lattice volume, i.e., lower crystalline density. A decrease in crystalline density [16] is partially related to inclusion of some side-chains by some authors (unlikely here for hexyl branches), and is usually associated with defects and reduced lamella thickness. Reduction in lamella/crystal thickness is indicated by a reduction in melting point (relation formally expressed through the well-known Thomson-Gibbs equation) and is thought to cause cell expansion due to surface dilatometric stresses, thermal

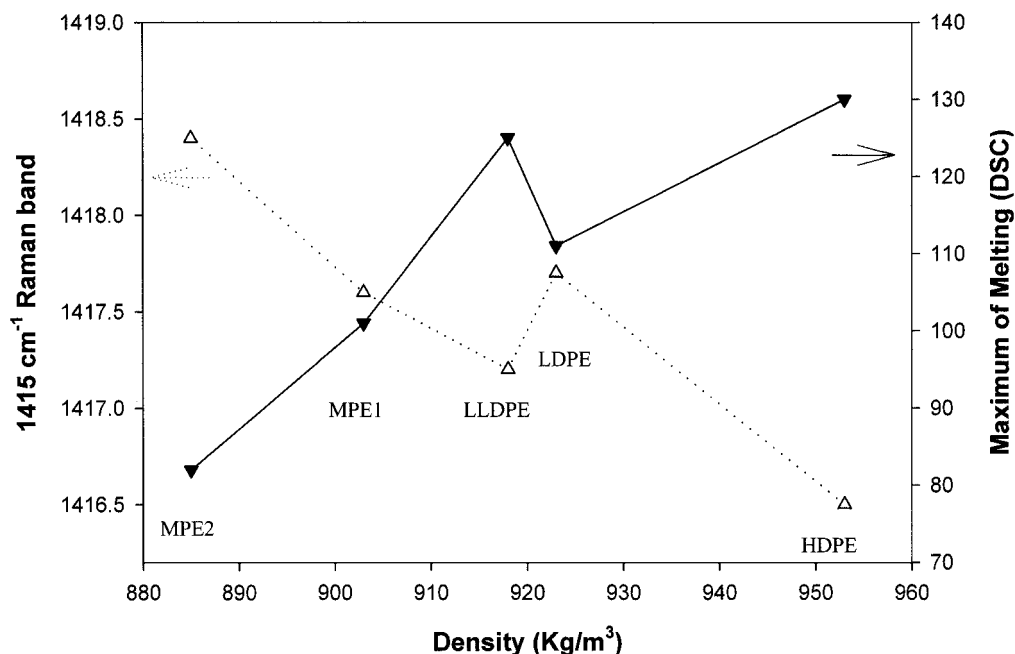


Figure 7 Position of the 1415 cm^{-1} Raman band (dotted line) and the maximum of melting (as measured by DSC) vs. polymer density for a number of polyethylene samples in Table I.

vibrations and intracrystalline defects resulting from faster crystallisation at the large undercoolings required. The fact that the cell expansion (crystalline density drop) in polyethylene is mostly due to the enlargement of the “*a*” cell parameter, parameter directly responsible for the lateral separation of the two interacting chains within the orthorhombic lattice, explains the change in splitting observed for the perpendicular to the chain direction $-\text{CH}_2-$ bending vibrational mode seen in Fig. 7. In fact, this interpretation is further supported by similar correlations found between the $-\text{CH}_2-$ bending factor group splitting separation of a family of orthorhombic aliphatic polyketones and their wide angle X-ray scattering crystalline density [17, 18].

Acknowledgements

Dr. B.J. Kip from DSM Research (The Netherlands) is acknowledged for fruitful discussions.

References

1. R. J. YOUNG, in “Introduction to Polymers” (Chapman and Hall, London, 1983) p. 157.
2. D. I. BOWER and W. F. MADDAMS, in “The Vibrational Spectroscopy of Polymers” (Cambridge University Press, New York, 1989).
3. J. M. LAGARON, A. K. POWELL and N. S. DAVIDSON, *Macromolecules* **33** (2000) 1030.
4. L. KURELEC, S. RASTOGI, R. J. MEIER and J. P. LEMSTRA, *ibid.* **33** (2000) 5593.

5. R. J. MEIER and A. VAN DER POL, *Vibrational Spectroscopy* **23** (2000) 95.
6. J. M. LAGARON, N. M. DIXON, W. REED, J. M. PASTOR and B. J. KIP, *Polymer* **40** (1999) 2569.
7. G. R. STROBL and W. HAGEDORN, *J. Polym. Sci., Polym. Phys. Ed.* **16** (1978) 1181.
8. C. C. NAYLOR, R. J. MEIER, B. J. KIP, K. P. J. WILLIAMS, S. M. MASON, N. CONROY and D. L. GERRARD, *Macromolecules* **28** (1995) 2969.
9. J. M. LAGARON, S. LOPEZ-QUINTANA, J. C. RODRIGUEZ-CABELLO, J. C. MERINO and J. M. PASTOR, *Polymer* **41** (2000) 2999.
10. F. J. BOERIO and K. L. KOENING, *J. Chem. Phys.* **52** (1970) 3425.
11. W. GLENZ, N. MOROSOFF and A. PETERLIN, *Polymer Letters* **9** (1971) 211.
12. W. GLENZ, A. PETERLIN and W. WILKE, *J. Polym. Sci.* **9** (1971) 1243.
13. T. SETO, T. HARA and K. TANAKA, *Jpn. J. Appl. Phys.* **7** (1968) 3.
14. M. E. VICKERS and H. FISHER, *Polymer* **36** (1995) 2667.
15. B. NEWAY, M. S. HEDENQVIST, V. B. F. MATHOT and U. W. GEDDE, *ibid.* **42** (2001) 5307.
16. P. R. HOWARD and B. CRIST, *J. Polym. Sci. Phys.* **27** (1989) 2269.
17. J. M. LAGARON, M. E. VICKERS, A. K. POWELL and N. S. DAVIDSON, *Polymer* **41** (2000) 3011.
18. J. M. LAGARON, M. E. VICKERS, A. K. POWELL and J. G. BONNER, *ibid.* **42** (2002) 1877.

Received 26 November 2001
and accepted 20 June 2002